

Direct comparison of visual cortex activation in human and non-human primates using functional magnetic resonance imaging

David J. Dubowitz^{a,*}, Dar-Yeong Chen^b, Dennis J. Atkinson^{c,1}, Miriam Scadeng^d,
Antigona Martinez^{e,2}, Michael B. Andersen^a, Richard A. Andersen^a,
William G. Bradley Jr^b

^a Division of Biology, 216-76, California Institute of Technology, Pasadena, CA 91125, USA

^b Long Beach MRI Center, Long Beach Memorial Medical Center, Long Beach, CA 90806, USA

^c Siemens Medical Systems R&D, Iselin, NJ 08830, USA

^d Department of Radiology, Los Angeles Children's Hospital, Los Angeles, CA 90027, USA

^e Department of Psychology, University of California, San Diego, La Jolla, CA 92093, USA

Received 7 August 2000; received in revised form 6 March 2001; accepted 6 March 2001

Abstract

We report a technique for functional magnetic resonance imaging (fMRI) in an awake, co-operative, rhesus macaque (*Macaca mulatta*) in a conventional 1.5T clinical MR scanner, thus accomplishing the first direct comparison of activation in visual cortex between humans and non-human primates with fMRI. Activation was seen in multiple areas of striate and extra-striate visual cortex and in areas for motion, object and face recognition in the monkey and in homologous visual areas in a human volunteer. This article describes T_1 , T_2 and T_2^* values for macaque cortex, suitable MR imaging sequences, a training schedule, stimulus delivery apparatus and restraining hardware for monkey fMRI using a conventional 19 cm knee coil. Much of our understanding of the functional organization of the primate brain comes from physiological studies in monkeys. Direct comparison between species using fMRI such as those described here will help us to relate the wealth of existing knowledge on the functional organization of the non-human primate brain to human fMRI. © 2001 Elsevier Science B.V. All rights reserved.

Keywords: MRI; fMRI; Functional activation; Human; Rhesus macaque monkey; Visual cortex; T_1 ; T_2 ; T_2^*

1. Introduction

This paper describes a novel application of functional magnetic resonance imaging (fMRI) for use in an awake-behaving macaque monkey, so that direct comparisons can now be made between rhesus macaque and human functional neuroanatomy. Suitable apparatus to position the monkey within the MRI scanner, and sequence parameters appropriate for macaque functional and anatomical imaging on a conventional

1.5T scanner are presented, as well as discussion on visual stimulus paradigms and animal handling and training. This report presents the first direct comparison of patterns of visual cortex activation between human and non-human primate species using fMRI under the same conditions, performing the same paradigm.

Since it is initial description (Ogawa et al., 1990), fMRI has seen much development in human subjects for psychology, neuroscience (Sereno et al., 1995; Tootell et al., 1995), and more recently for clinical applications (Stapleton et al., 1997; Lee et al., 1999), allowing us to delineate areas of functional deficit (rather than merely structural deficit) or to track functional recovery (Bilecen et al., 2000). The technique produces images of activated brain regions by detecting the indirect effect of neural activity on local blood flow and oxygen saturation — the Blood Oxygen Level Dependent effect or BOLD.

* Corresponding author. Tel.: +1-626-3958337; fax: +1-626-7952397.

E-mail address: dubowitz@vis.caltech.edu (D.J. Dubowitz).

¹ Present address: GE Medical Systems, Western Region, 7, Foxglove Way, Irvine, CA 92612.

² Present address: Sackler Institute of Weill Medical College, Cornell University, New York, NY 10021.

The application of fMRI has advanced ahead of our understanding of the underlying physiological activities we are studying. fMRI appears to be related to spiking activity of large ensembles of neurons and to local field potentials. The ability of fMRI to represent the population activity of whole ensembles of neurons is a significant contribution to the study of neurophysiology (Paradiso, 1999; Disbrow et al., 2000; Logothetis et al., 2000; Rees et al., 2000) and could consequently improve the efficacy of human fMRI as a neuroscience and clinical tool. Macaques are readily trained to perform complex tasks, and with the aid of microelectrode mapping, radioisotope tracers and anatomical studies, have formed the basis of much of our current understanding about primate visual pathways (Maunsell and Newsome, 1987; Tootell et al., 1988; Felleman and Van Essen, 1991; Andersen, 1997; Snyder et al., 1997). Earlier studies have addressed the potential value of fMRI in awake macaque monkeys for investigating visual neuroscience (Dubowitz et al., 1998; Stefanacci et al., 1998; Logothetis et al., 1999; Paradiso, 1999) and basal ganglia function (Zhang et al., 2000). Evaluating the BOLD effect and correlating it with the underlying neural event is a complex process. Earlier approaches have involved co-registration of event related potentials (ERP), magnetoencephalography (MEG) and electroencephalography (EEG) data with fMRI (George et al., 1995; Martinez et al., 1999) which helps elucidate the underlying temporal trends, but lacks spatial specificity. Another approach has been to compare neural activity in monkeys with functional MRI in humans, however, this often proves confusing as both inter-species and inter-technique variability need to be considered (Tootell et al., 1996; Heeger et al., 2000; Rees et al., 2000). Using a monkey model for fMRI (Dubowitz et al., 1998) would bridge this gap in two ways — firstly, allowing comparison of behavioral electrophysiological and fMRI changes in the same animal (direct comparison of fMRI with electrophysiological recordings in humans being limited ethically to cases with preexisting pathology). Secondly, the ability to make direct comparisons between the human and macaque brain using the same imaging technique, and while performing the same paradigm has the potential to greatly improve our understanding of the human brain, allowing us to make direct inferences about human neurophysiology based on our existing wealth of knowledge from macaque neurophysiology.

2. Materials and methods

2.1. Experimental set-up

2.1.1. Animal studies

All animal studies were performed in a healthy, 6.5 kg,

adolescent 5-year-old male rhesus macaque. Approval for this research was obtained from The Institutional Animal Care and Use Committee, Epidemiology and Biosafety Committees. The monkey was trained to lie prone with his head erect ('sphinx' position) in the bore of a clinical MR scanner and to look at a viewing screen placed 200 cm in front of him. The monkey's head was held motionless for the duration of the experiment by means of a surgically attached MR compatible plastic head-cap. To minimize susceptibility artifacts from the restraint, this was machined from a single piece of polyetherimide resin (a material having both good biocompatibility and susceptibility close to that of tissue). The monkey was transported to the MRI facility in a MRI compatible transport cage. An acrylic (Plexiglas) tube was attached to the transport cage, and the monkey then crawled into the tube, from which only his head protruded. The acrylic tube containing the monkey was then positioned in the MRI scanner (Fig. 1), and the head cap was secured to the window in the receive/transmit coil. This allowed the head to be restrained during experiments, but could be loosened to allow the monkey to raise or lower his head freely between experiments. A tube to supply fruit juice was positioned near the mouth to reward the monkey at the conclusion of each experiment. The monkey wore a diaper for the duration of the study, and all areas of the MRI scanner with which the monkey could come into contact (MR table, RF coil) were covered in polythene sheeting. Initial training consisted of habituating the animal to a travel cage, and teaching him to crawl into an acrylic tube (taking ca. 2 months). Subsequent training was performed both in a mock-up of the MRI environment and in the MRI scanner to reward the monkey for keeping still while viewing a visual stimulus (taking ca. 6 months). Rewarding the monkey consisted of positive re-enforcement with treats the monkey enjoyed (in this particular case, fruit juice). Even with head fixation, the monkey was able to move up to 2 or 3 mm. Good behavioral control and the willing co-operation of the monkey was essential to obtain images free from motion artifacts.

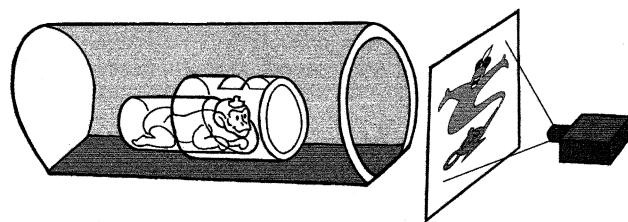


Fig. 1. The monkey lies within the MRI in a sphinx position in the RF knee coil. A visual stimulus is provided by a video projector on a screen at the opening to the MRI bore.

2.1.2. Human studies

A young adult male (17-year) was used as an adolescent 'age matched' human control. Informed consent, following Institutional Review Board ethical guidelines, was obtained after detailed explanation of the procedure. The subject lay supine, and viewed the same paradigm as the monkey on the screen at his feet via a mirror attached to the head coil (ensuring the same viewing distance and visual field of view as the monkey). His head was restrained with foam pads.

2.2. Choice of stimulus

Macaques, like humans have a very advanced visual system and use this as their primary sense. For this study, a global stimulus, which would elicit responses in many parts of the visual pathways was required, and to which the monkey would readily attend. Preliminary observations were made on two adult male macaques while they watched movie videos in the laboratory to elucidate what sort of visual stimulus would best hold a monkey's attention. Comparison was made between white noise, monochrome movies, color movies and animated cartoons. Attention was judged by recording maximal fixation times. Macaques showed a clear preference for animated cartoons, for which they were capable of maintaining attention, with intermittent short gaps, for up to 35 min. They are easily distracted, and a noisy, colorful movie and a regular reward system greatly improves their performance.

2.3. Stimulus paradigm

A visual stimulus was provided using a LCD video projector. For the experiments presented here, sequences from a child's animated film were presented to the monkey in 24 s clips. The film was chosen to include rapidly changing colors, contrast levels, faces and movement. Each film clip was preceded by a period of complete darkness for 24 s. The 48-s cycle was repeated three times with an additional period of 24 s darkness at the end. The whole sequence lasted 3.5 min and was repeated four times (for signal averaging). For the data presented in this report, the monkey was required only to look passively at the screen. The human subject viewed the same stimulus, but due to superior signal-to-noise ratio (SNR) in fMRI of human brain, only two repetitions were needed.

2.4. MR system

All imaging was performed on a conventional 1.5 T Siemens VISION MR scanner equipped with 25 mT/m gradients (300 μ s rise times). A 19 cm circularly polarized knee coil was used as this was found to have the optimal loading characteristics and 50–100% superior-

ity in SNR over a conventional head coil or flexible surface coil (Dubowitz et al., 1998). The monkey's head was positioned at the center of the radio frequency (RF) coil. This provided maximum SNR despite the resulting asymmetrical coil loading by the animal's torso. Local shimming was with an experimental volume-shim algorithm (Heid, 1996).

In order to optimize anatomical and BOLD weighted sequences for monkey cortex, T_1 , T_2 and T_2^* relaxation times were measured in gray and white matter. A phase-sensitive inversion recovery (IR) sequence was used for T_1 measurements (repetition time (TR), 7666 ms, echo time (TE), 29 ms, inversion times (TI), 300, 450, 600, 900, 1200, 1500 ms). A 2D Fast Low Angle Shot (FLASH) sequence was used to measure T_2^* (TR 1000 ms, TE 5, 7, 10, 12, 15, 18, 20 ms) and T_2 measured by fitting alternate echoes of a Carr–Purcell–Meiboom–Gill (CPMG) multiecho spin echo sequence (TR 8000 ms, TE 22.5 ms–360 ms in 22.5 ms intervals). Five slices were acquired with 200 \times 200 mm FOV and a 256 \times 256 matrix with a slice thickness of 5 mm (parameters are summarized in Table 1).

Anatomical imaging was obtained using a 3-D Magnetization-Prepared Rapid Gradient Echo (MPRAGE) sequence. The measured T_1 values of monkey cortex were used to set initial sequence parameters. The sequence was then further refined empirically for best gray/white matter contrast. Optimal parameters for monkey cortex were found to be TR/TE = 11.4/4.4 ms, flip angle 12°, inversion time (preparation time) 250 ms and delay time (magnetization recovery time) 600 ms. A 90 \times 90 mm field of view (FOV) was acquired with a 128 \times 128 matrix, and 98 phase encode steps made through a 80 mm slab (0.7 \times 0.7 \times 0.8 mm resolution). 100% over-sampling was used in the phase, read and slab directions to reduce 'wrap' artifacts and increase SNR. The total acquisition time was 13 min.

For BOLD weighted images, a low bandwidth (833 Hz per pixel) echo-planar gradient echo (EPI GE) sequence was found to give the best results (SNR from echo-planar spin echo was observed to be too low at 1.5 T for monkey fMRI). Echo planar images were collected in the x-y plane within the scanner (i.e. coronal in the prone monkey, and transaxial in the supine human subject) this choice of scan-plane took advantage of the most homogeneous B_0 field direction and minimized EPI warping artifacts. The effective echo time (TE_{eff}) of 40 ms was chosen to approximate the T_2^* of monkey cortex for maximal functional contrast (Bandettini et al., 1993). Eight, 5 mm thick coronal slices of the monkey's occipital cortex were acquired per repetition of 2000 ms, thus the effective TR = 2000 ms. Eighty-six repetitions of the eight slices were acquired, the whole run taking less than 4 min. The first two repetitions were not used in data analysis allowing 4 s (4-times T_1 of gray matter) to ensure steady state.

Table 1
Summary of MRI sequence parameters for fMRI anatomical and relaxation measurements

Sequence	Anatomy (human)	Anatomy (monkey)	BOLD (human)	BOLD (monkey)	T_1 (monkey)	T_2 (monkey)	T_2^* (monkey)
	3D-MPRAGE	3D-MPRAGE	EPI-GE	EPI-GE	True IR	CPMG	2D-FLASH
Bandwidth (Hz) ^a	33 280 (130)	16 640 (130)	106 624 (833)	106 624 (833)	33 280 (130)	33 280 (130)	33 280 (130)
Echo time, TE (ms)	4.4	4.4	40	40	29	22.5–360	5–20
Repetition time, TR (ms)	11.4	11.4	2000 ^b	2000 ^b	7666	8000	1000
Inversion time, TI (ms)	20	250	–	–	300–1500	–	–
Delay time, TD (ms)	0	600	–	–	–	–	–
Flip angle (°)	10	12	90	90	180	90	90
Number of averages	1	1	1	1	1	1	1
Field of view, FOV (mm)	256 × 256	90 × 90	448 × 448	256 × 256	200 × 200	200 × 200	200 × 200
Imaging matrix	256 × 256	128 × 128	128 × 128	128 × 128	256 × 256	256 × 256	256 × 256
Imaging plane	Sagittal	Axial	Axial	Coronal	Axial	Axial	Axial
Slice (slab) Thickness (mm)	140 ^c	80 ^c	4	5	5	5	5
Number of slices	140 ^d	98 ^d	–	–	5	5	5
Voxel resolution (mm)	1 × 1 × 1	0.7 × 0.7 × 0.8	3.5 × 3.5 × 4	2 × 2 × 5	0.8 × 0.8 × 5	0.8 × 0.8 × 5	0.8 × 0.8 × 5
Number of measurements ^e	–	–	84 × 2	84 × 4	–	–	–

^a Bandwidth per pixel shown in parentheses.

^b Effective TR determined by the fMRI experiment repetition time.

^c Slab thickness is shown for 3D sequences.

^d Indicates number of phase encode steps for 3D sequence.

^e Number of time points measure × number of experiments averaged.

Optimum voxel size for macaque was determined empirically to allow maximum BOLD contrast-to-noise ratio (CNR) per pixel without excessive partial volume averaging (Dubowitz et al., 1998). A voxel volume of 40 μ l provided optimal BOLD CNR but was too coarse to define anatomical structures in the small macaque brain. Resolution was improved to 20 μ l and SNR elevated with use of four-fold signal averaging. This resolution was achieved by imaging a FOV of 256 × 256 mm and a 128 × 128 matrix using 5 mm slices (resolution 2 × 2 × 5mm).

For the human studies, a conventional circularly polarized 26 cm head coil was used. Optimum sequence timing parameters for 3D-MPRAGE were TR/TE = 11.4/4.4 ms, flip angle 10°, inversion time 20 ms and delay time 0ms. A 256 × 256 mm FOV and 256 × 256 matrix was acquired, and 140 phase encode steps taken through a 140 mm slab (isotropic 1 mm resolution). The sequence had been earlier optimized for another human fMRI study, and was not re-optimized in this current study (Martinez et al., 1999). For BOLD studies the same low bandwidth (833 Hz per pixel) was used with $TE_{\text{eff}} = 40$ ms, and effective TR = 2000 ms. Then, 10 axial 4 mm slices with FOV 448 × 448 mm were acquired every 2000 ms with a 128 × 128 matrix to achieve the desired voxel size (resolution 3.5 × 3.5 × 4 mm). Eighty-six repetitions of the ten slices were taken in under 4 min (84 used for image processing). This was

repeated twice for signal averaging. Image parameters are summarized in Table 1.

2.5. Image post-processing

The time-dependent echo-planar images were processed off line on a Sun/Sparc unix workstation with AFNI software (Cox and Hyde, 1997). Time series were initially corrected for any motion using a reregistration technique and Fourier interpolation within AFNI. The multiple repetitions of the time-dependent series (four for the monkey studies, two for the human studies) were averaged into a single series to improve SNR. Functional images were generated using a cross-correlation technique. A series of phase-shifted trapezoids were used as the reference waveforms, which were cross-correlated on a pixel-by-pixel basis with the MR signal time course. Gram-Schmidt orthogonalization was used to remove drift in the time series using a third order polynomial (Bandettini et al., 1993). To remove spurious pixels, the functional intensity map was thresholded at a correlation-coefficient value of $|r| > 0.5$ ($P < 1 \times 10^{-3}$ following conservative Bonferroni correction for multiple comparisons). Only pixels in a cluster of at least three contiguous significant pixels were displayed. Functional images were generated by fitting the reference waveform to the MR signal time

course by linear fit, with intensity representing the magnitude of the fit coefficient. To reject spurious activation in areas of low signal, the linear fit coefficient was normalized by the baseline MR signal for each pixel. Pixel intensity was thus calibrated as percentage change relative to baseline. MPRAGE and functional maps were co-registered using AFNI software. Discrepancies in the co-registration were corrected by ‘nudging’ the anatomical images (up to one or two pixels). Images were treated as rigid bodies and no unwarping performed. No additional interpolation or resampling was performed. Studies with residual motion artifact, which was not corrected by image re-registration were rejected. This was assessed by examining the MR time course of areas of scalp which would be sensitive to stimulus correlated motion artifact — but would not be expected to have stimulus-correlated BOLD activation.

Borders of functional cortical areas in human brain were defined by areas of significant activation during the fMRI task, and subdivided manually based on earlier human fMRI literature (Serenio and Allman, 1991; DeYoe et al., 1994; Serenio et al., 1995; Howard et al., 1996; Tootell et al., 1996; Kanwisher et al., 1997; Clark et al., 1998; Serenio, 1998; Gauthier et al., 1999) and PET literature (Zeki et al., 1991; McKeefry et al., 1997). In the macaque, areas of activation were manually subdivided into distinct retinotopic cortical regions from anatomical studies (Tootell et al., 1988; Paxinos et al., 1999) and single unit recording and tracer studies (Gattass et al., 1981; Ungerleider and Desimone, 1986; Gattass et al., 1988; Boussaoud et al., 1991).

Post-processing of spin-echo and gradient-echo images for tissue relaxometry in macaque brain was done using NIH-Image software (US National Institutes of Health, <http://rsb.info.nih.gov/nih-image/>). Multiple regions of interest (ROI) were drawn around anatomically defined gray and white matter on the TI = 300 ms phase-sensitive IR images (which had the best gray/white matter contrast) and the ROI copied to all the other images. To calculate T_1 values, MR signal intensity $S(TI)$ for gray matter and white matter was fitted to the inversion-recovery relaxation curve described by Eq. (1):

$$S(TI) = M_0(1 - e^{-TI/T_1}) + M_z(0)e^{-TI/T_1} \quad (1)$$

Where M_0 is the initial longitudinal magnetization, $M_z(0)$ is the magnetization at TI = 0, immediately following the inversion pulse and TI is the inversion time.

T_2 values were calculated from the CPMG sequence by fitting the MR signal $S(n\tau)$ in gray and white matter to alternate echoes of the spin-echo relaxation curve described in Eq. (2):

$$S(n\tau) = \begin{cases} S_{\text{ODD}}e^{-n\tau/T_2}(1 - e^{-TR/T_1}) & n = 1,3,5,7,\dots \\ S_{\text{EVEN}}e^{-n\tau/T_2}(1 - e^{-TR/T_1}) & n = 2,4,6,8,\dots \end{cases} \quad (2)$$

τ is the CPMG echo spacing (22.5 ms), n is the echo number, S_{ODD} and S_{EVEN} are the initial signals at $n=0$ for the odd and even echo trains, respectively. The final value for T_2 was the mean of T_2 values calculated from even and odd echo relaxation curves.

T_2^* values were calculated by assuming an exponential relationship between the MR signal, $S(TE)$, and the echo time, TE, described by Eq. (3):

$$S(TE) \approx S'(0)e^{-TE/T_2^*} \quad (3)$$

$S'(0)$ is the initial signal at TE = OL.

The fit optimization was implemented in Matlab (The Mathworks Inc., Natick, MA) using a proprietary large-scale subspace trust-region algorithm based on an interior-reflective Newton method (Coleman and Li, 1996). The algorithm allows specification of upper and lower bounds on each optimized parameter.

3. Results

Measured values of T_1 and T_2 relaxation times for macaque cortex are shown in Table 2. The T_2 values of Macaque gray matter were lower than in humans, and the T_1 values higher. White matter results were identical for both species. These T_1 and T_2^* values were used as a first approximation in optimizing the MPRAGE and BOLD weighted sequences, respectively, as described above.

The functional intensity maps for macaque and human visual cortex show homologous anatomical locations in both species and have been labeled in Fig. 2 Fig. 3. Areas of fMRI activation are clearly seen as discrete areas in the striate and extra-striate visual cortex. These show high correlation with the presented visual stimulus. Activation is observed in the

Table 2

T_1 , T_2 and T_2^* values for macaques brain in $n = 3$ monkeys expressed as mean \pm standard deviation (S.D.)^a

	Gray matter ($n = 3$)	White matter ($n = 3$)
T_1 (ms)	1010 \pm 8.5 (920)	790 \pm 4.0 (790)
T_2 (ms)	94 \pm 0.8 (101)	92 \pm 2.5 (92)
T_2^* (ms)	49 \pm 2.3	46 \pm 6.5

^a Typical values for human brain are shown in parentheses (Wood et al., 1993).

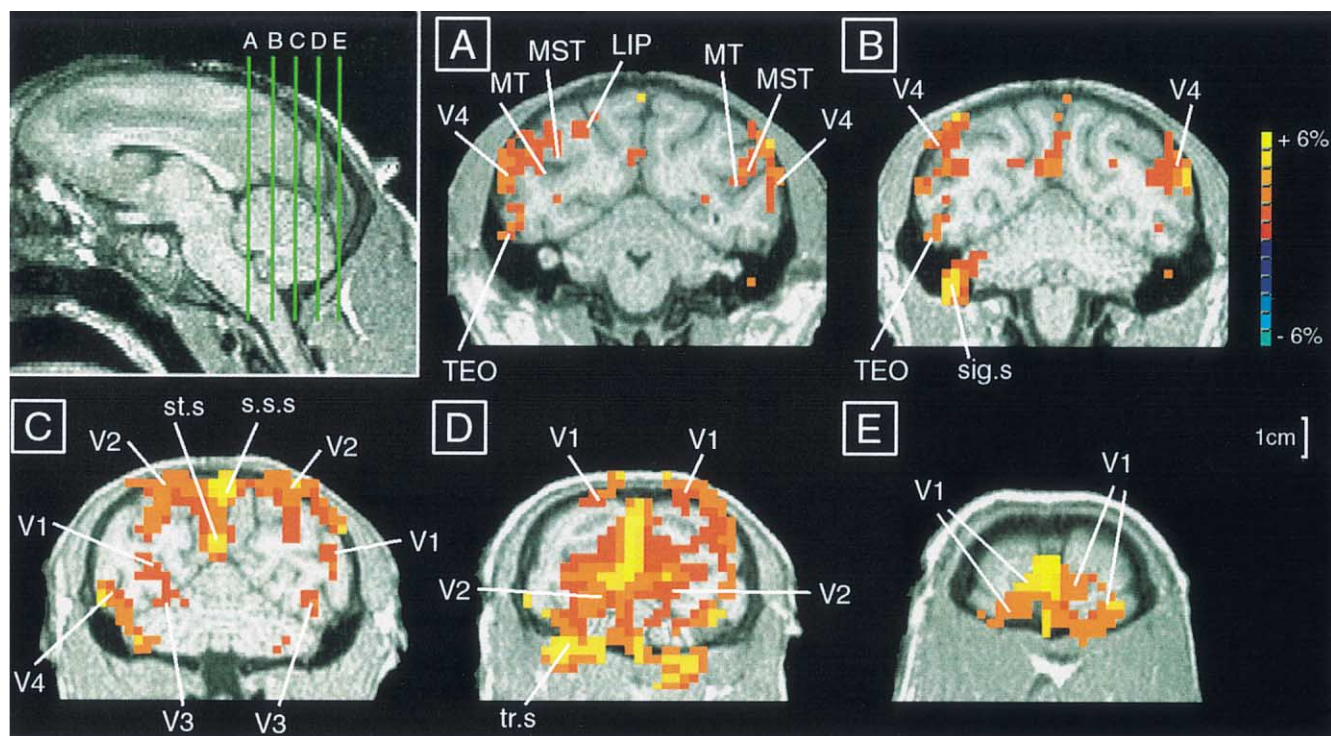


Fig. 2. Functional activation in macaque brain. Activated pixels are 2×2 mm superimposed on T_1 weighted MP-RAGE images of 0.7×0.7 mm resolution (coronal images A–E are at 5 mm spacing ranging from 25 to 5 mm anterior to the occipital pole). Labeled areas are visual cortex (V1, V2, V3, V4), medial temporal area (MT), medial superior temporal area (MST), lateral intraparietal area (LIP), superior sagittal sinus (s.s.s), straight sinus (st.s), transverse sinus (tr.s), sigmoid sinus (sig.s).

macaque brain in areas corresponding to hierarchical visual cortical areas V1, V2, V3, V4, in parietal area LIP (lateral intraparietal) and temporal areas MT (medial temporal), MST (medial superior temporal) and TEO (temporal occipital area). The central veins draining this area (superior sagittal sinus, straight sinus, transverse sinus and sigmoid sinus) also show activation. Human cortical activation is seen in homologous visual areas V1, V2, VP, V3A, V4, MT-complex (MT+), fusiform, lingual and parahippocampal gyri and anterior visual motion areas.

4. Discussion

This technique provides high resolution images of discrete areas of fMRI activation in the macaque monkey, which are comparable to visual fMRI studies in humans. Areas of activation are recognizable in striate and extra-striate visual cortex consistent with what would be expected from this global stimulus paradigm.

The strong activation in the primary and secondary areas (V1, V2) of macaque retinotopic visual cortex (Fig. 2) confirms the cartoon movie is stimulating visual pathways. Activation is also noted in ventral and

dorsal visual processing streams. This includes area V4 (associated with the vivid colors in a stimulus) (Zeki, 1973), also noted is activation in areas V3 and medial temporal area, MT, which are associated with the perception of moving scenes in a stimulus (Felleman and Van Essen, 1987). Activation in medial superior temporal area, MST, suggests that the stimulus may be providing 'optic flow' (the complex visual motion that may be encountered during self-motion) (Saito et al., 1986; Tanaka et al., 1986). Activation of TEO (architectonic temporal occipital area) has previously been associated with object and face recognition (Bousaoud et al., 1991) and fMRI activation in area TEO seen in this experiment may indicate that the monkey is recognizing faces and distinct objects in the cartoon. Activation located in the lateral intraparietal area, LIP, is seen with stimuli requiring saccadic movements to different areas of interest on the screen (Gnadt and Andersen, 1988) (i.e. a non-fixating stimulus).

The activation in the human visual cortex shows a similar pattern of retinotopic cortical activation, with ventral and dorsal stream activation. The anatomical positions do not correlate structurally across species (Sereno and Allman, 1991; Tootell et al., 1996; Sereno, 1998), however, functionally homologous areas of activation are identified in both species, and their relative

size and position are readily observed. Retinotopic visual areas V1, V2 and VP are activated during the stimulus (Fig. 3). Human visual cortex also shows V4 activation, which may be associated with the vivid colors of a stimulus (Zeki et al., 1991) and activation in the MT-complex (the human homologue of macaque area MT and MST) similar to that seen in the monkey (Tootell et al., 1995). Comparison with previous studies of face and object recognition in humans show similar patterns of cortical activation in the lingual and fusiform gyri (Kanwisher et al., 1997; Clark et al., 1998; Gauthier et al., 1999) using the current stimulus. These are believed to be homologous to macaque area TEO (Kanwisher et al., 1997). Activation in human supplementary anterior visual motion areas is also observed adjacent to auditory cortex, which may correspond to the macaque superior temporal polysensory area (Howard et al., 1996). Although the stimulus activated many areas of the visual pathways, the exact feature of the stimulus (e.g. color, motion, objects) that is actually activating each distinct area in macaque or human cortex is not confirmed from the current study and is the subject of ongoing work. These initial observations of areas of potential cross species homology are currently the subject of more detailed fMRI studies with more directed stimuli than the simple cartoon animation described here.

There are asymmetries in the patterns of visual activation in both the macaque and human fMRI studies. Functional lateralization is well described in humans—particularly language, parietal function and dominant handedness. fMRI studies have described lateral asymmetry in other areas—e.g. MT-complex (Howard et al., 1996). Unlike human studies the macaques fMRI does not show any lateral asymmetry in MT activation. This is not unexpected, as clinically, Macaques show considerably less lateralization than humans (and are ambidextrous). Despite this, some asymmetry is seen in the pattern of activation in the macaque (e.g. dorsal V1 in Fig. 2d). This may be due to the stimulus used. The subject was free to observe the movie without fixating at a particular part of it, thus it is possible that both the monkey and human subjects experienced fluctuations in visual attention, perhaps becoming less attentive to all or part of the stimulus. Visual attention has been shown to modulate fMRI signal in retinotopic visual cortex (Martinez et al., 1999). Further studies are planned which include a more refined stimulus paradigm to more precisely map known areas of cerebral activation. For these more complex paradigms and for behavioral studies, we have developed an infrared system for real-time monitoring of eye position, which will enable us to better answer these questions.

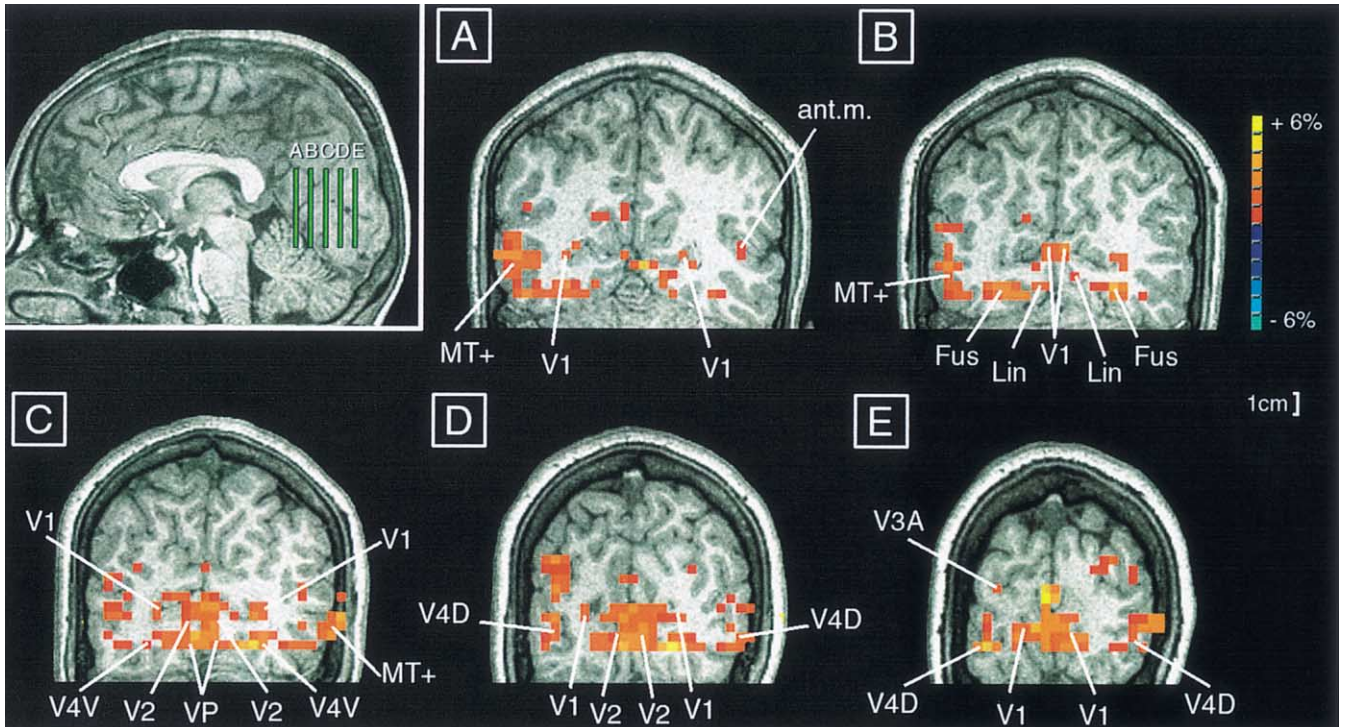


Fig. 3. Functional activation in human visual cortex. Activated pixels are 3.5×4 mm superimposed on T_1 weighted MP-RAGE images of 1 mm isotropic resolution. Coronal images A–E are at 7 mm spacing ranging from 44 to 16 mm anterior to the occipital pole. Green bars on the sagittal image indicate the position of coronal images A–E (height of green bars indicates superior-inferior extent over which fMRI data was acquired). Labeled areas are visual cortex (V1, V2, VP, V3A, V4-dorsal and ventral), medial temporal complex (MT+), fusiform gyrus (Fus), lingual gyrus (Lin), anterior motion area (ant.m).

The imaging parameters used to generate these fMRI images of macaque cortex result in a pixel dimension approximating the cross sectional diameter of the large draining cerebral veins. This tends to exaggerate the signal from these structures, as does our use of a gradient echo EPI sequence for BOLD imaging. These structures are readily apparent in Fig. 2 (superior sagittal sinus, straight sinus, transverse sinus, and sigmoid sinus). They are easily differentiated from activation in adjacent cortical structures by their anatomical position. Measures to suppress the signal from larger veins (spin echo EPI, diffusion weighting, smaller voxels) would result in lower signal to noise and reduced fMRI sensitivity. Any anatomical ambiguity was felt to be minimal, and was outweighed by the overall improved BOLD CNR. Large draining veins are not seen in the human study because the ten axial slices were centered at the level of the visual cortex and did not extend sufficiently superiorly to include the midline sinuses.

Due to the small overall size of the monkey brain, and the smaller detail with which it needs to be examined, both resolution and SNR need to be maximized. Empirically a voxel size between 30 and 45 μl was preferred, providing both adequate SNR and BOLD CNR (Dubowitz et al., 1998). This resolution was, however, found to be too coarse to define anatomical structures in the small macaque brain. Signal averaging allows some compromise in SNR per run to achieve better resolution (four averages of a 20 μl have the same effective SNR as a 40 μl voxel).

The percentage modulation provides a useful benchmark when comparing the animal model with human studies, but is not a good measure for optimizing voxel sizes (Dubowitz et al., 1998). CNR increases with increasing voxel size, but the baseline MRI signal may also change due to partial volume averaging. With smaller voxels CNR is reduced. Reducing the in-plane resolution at the expense of some through-plane resolution also allowed reduction of susceptibility artifacts from surrounding hardware while retaining overall voxel size and SNR. As with all NMR experiments, this represents a compromise, and the larger through-plane slice profile results in a 'stair-case' approximation to the posterior curvature of the brain. Thus some cortical pixels are projected beyond the apparent margin of the brain when superimposed on the high-resolution anatomical images (even though they are clearly within cortex on the raw echo planar images). Improvement in through-plane resolution can be achieved with further repetition and averaging, but this also prolongs the time which the monkey must remain still in the scanner. The parameters described above represent a good compromise in which some trade-off is necessary to retain subject concentration and co-operation. With further training and habituation further improvement is anticipated.

Relaxometry studies of macaque brain show that gray matter T_1 relaxation is longer than human gray matter and T_2 relaxation slightly shorter than human gray matter. White matter values are identical in both species (Table 2). T_2 relaxation time reduces with increasing neuronal organization (e.g. T_2 trend in fetal vs. neonatal vs. adult brain) (Barkovich, 2000). The comparable T_2 times may indicate a level of structure and organization comparable to human cortex. These results differ from earlier values (Dubowitz et al., 1998), and we believe are more accurate as the current technique uses a more rigorous methodology and also incorporates $n = 3$ animals. A CPMG multi echo method was used which has been shown to give a superior measurement for T_2 compared with conventional spin echo (Carr and Purcell, 1954; Meiboom and Gill, 1958). In addition the alternate echoes were fitted separately to compensate for possible shortfalls in the 180° pulse and eddy current effects. The exponential fit for the phase sensitive IR sequence also used a fit parameter for the 180° pulse, to allow for shortfalls in the flip angle in different tissues. The curve fitting algorithm used in this study was also superior to that used earlier (Dubowitz et al., 1998) and now incorporates a large-scale subspace trust-region algorithm and allows specification of upper and lower bounds on each optimized parameter which achieves superior convergence. The current results suggest human and macaque relaxation parameters are closer to each other than was previously thought.

Monkey imaging has been achieved using a standard Siemens RF volume knee coil. This was found to provide the best SNR characteristics for imaging monkeys. It also provided a convenient anchor point for our head-post locator. While surface coils may improve signal-to-noise in imaging the occipital cortex, other practical matters precluded their use; the large size of the standard flex coil (37×17 cm) made it more difficult to use with monkeys and homogeneous coverage of the whole brain was better with the volume coil. This ability to utilize the manufacturer's standard equipment makes this experimental model versatile. Monkey MRI can be achieved using a clinical scanner and standard clinical knee coil without the necessity or expense of building dedicated RF hardware.

5. Conclusion

This technique produces high quality fMRI images in *Macaca Mulatta* visual cortex using a conventional 1.5 T clinical MR scanner and a standard RF volume coil and allows direct comparison with human fMRI. The stimulus paradigm used is simple, and non-interactive. It activates large areas of striate and extrastriate visual cortex. The results of this study demonstrate that fMRI

data from a macaque monkey can be used as a model for studying the physiology of fMRI in man. The T_1 and T_2 values of macaque brain are similar to humans, and the functional distribution of activation in the visual pathways also appear to be homologous. The existing wealth of understanding of functional organization in macaque cortex can now be more directly correlated with emerging data from human fMRI studies. The basic technique can be easily modified to allow imaging of other areas of the macaque cortex, permitting further comparison with humans.

The technique described here represents a new tool for studying the underlying physiology of functional MRI using a method, which can be implemented on any conventional clinical MRI scanner. The true strength of this model will be combining this cross-species fMRI study with animal fMRI and direct electrophysiological studies. This would give us a much better handle on the significance of fMRI activation maps in humans with respect to the underlying neuronal activity. This understanding is one of the next crucial steps in refining fMRI as a neuroscience and clinical tool.

Acknowledgements

We thank Chris Headrick for the illustration (Fig. 1), Betty Gillikin for animal care assistance and Marty Sereno for enlightening discussion and assistance with data interpretation. This work is supported by grants from the Pasadena Neurosciences Fellowship of Huntington Medical Research Institutes (DJD) and the National Eye Institute (RAA).

References

Andersen RA. Neural mechanisms of visual motion perception in primates. *Neuron* 1997;18:865–72.

Bandettini PA, Jesmanowicz A, Wong EC, Hyde JS. Processing strategies for time-course data sets in functional MRI of the human brain. *Magn Reson Med* 1993;30:161–73.

Barkovich AJ. *Pediatric Neuroimaging*, Third ed. Philadelphia: Lippincott Williams and Wilkins, 2000.

Bilecen D, Seifritz E, Radu EW, Schmid N, et al. Cortical reorganization after acute unilateral hearing loss traced by fMRI. *Neurology* 2000;54:765–7.

Boussaoud D, Desimone R, Ungerleider LG. Visual topography of area TEO in the macaque. *J Comp Neurol* 1991;306:554–75.

Carr HY, Purcell EM. Effects of diffusion on free precession in nuclear magnetic resonance experiments. *Phys Rev* 1954;94:630.

Clark VP, Maisog JM, Haxby JV. fMRI study of face perception and memory using random stimulus sequences. *J Neurophysiol* 1998;79:3257–65.

Coleman TF, Li Y. An interior trust region approach for nonlinear minimization subject to bounds. *SIAM J Optim* 1996;6:418–45.

Cox RW, Hyde JS. Software tools for analysis and visualization of fMRI data. *NMR Biomed* 1997;10:171–8.

DeYoe EA, Bandettini P, Neitz J, Miller D, Winans P. Functional magnetic resonance imaging (fMRI) of the human brain. *J Neurosci Methods* 1994;54:171–87.

Disbrow EA, Slutsky DA, Roberts TP, Krubitzer LA. Functional MRI at 1.5 tesla: a comparison of the blood oxygenation level-dependent signal and electrophysiology. *Proc Natl Acad Sci USA* 2000;97:9718–23.

Dubowitz DJ, Chen DY, Atkinson DJ, Grieve KL, et al. Functional magnetic resonance imaging in macaque cortex. *Neuroreport* 1998;9:2213–8.

Felleman DJ, Van Essen DC. Receptive field properties of neurons in area V3 of macaque monkey extrastriate cortex. *J Neurophysiol* 1987;57:889–920.

Felleman DJ, Van Essen DC. Distributed hierarchical processing in the primate cerebral cortex. *Cereb Cortex* 1991;1:1–47.

Gattass R, Gross CG, Sandell JH. Visual topography of V2 in the macaque. *J Comp Neurol* 1981;201:519–39.

Gattass R, Sousa AP, Gross CG. Visuotopic organization and extent of V3 and V4 of the macaque. *J Neurosci* 1988;8:1831–45.

Gauthier I, Tarr MJ, Anderson AW, Skudlarski P, Gore JC. Activation of the middle fusiform ‘face area’ increases with expertise in recognizing novel objects. *Nat Neurosci* 1999;2:568–73.

George JS, Aine CJ, Mosher JC, Schmidt DM, et al. Mapping function in the human brain with magnetoencephalography, anatomical magnetic resonance imaging, and functional magnetic resonance imaging. *J Clin Neurophysiol* 1995;12:406–31.

Gnadt JW, Andersen RA. Memory related motor planning activity in posterior parietal cortex of macaque. *Exp Brain Res* 1988;70:216–20.

Heeger DJ, Huk AC, Geisler WS, Albrecht DG. Spikes versus BOLD: what does neuroimaging tell us about neuronal activity? *Nat Neurosci* 2000;3:631–3.

Heid OH. Noniterative localized in vivo shimming in < 15s. *Proc Int Soc Magn Res Med* 1996;1:363.

Howard RJ, Brammer M, Wright I, Woodruff PW, et al. A direct demonstration of functional specialization within motion-related visual and auditory cortex of the human brain. *Curr Biol* 1996;6:1015–9.

Kanwisher N, McDermott J, Chun MM. The fusiform face area: a module in human extrastriate cortex specialized for face perception. *J Neurosci* 1997;17:4302–11.

Lee CC, Ward HA, Sharbrough FW, Meyer FB, et al. Assessment of functional MR imaging in neurosurgical planning. *Am J Neuroradiol* 1999;20:1511–9.

Logothetis NK, Guggenberger H, Peled S, Pauls J. Functional imaging of the monkey brain. *Nat Neurosci* 1999;2:555–62.

Logothetis NK, Pauls J, Oeltermann A, Trinath T, Augath M. The relationship of LFPs, MUA and SUA to the BOLD fMRI signal. *Proc Soc Neurosci* 2000;26:820.

Martinez A, Anillo-Vento L, Sereno MI, Frank LR, et al. Involvement of striate and extrastriate visual cortical areas in spatial attention. *Nat Neurosci* 1999;2:364–9.

Maunsell JH, Newsome WT. Visual processing in monkey extrastriate cortex. *Annu Rev Neurosci* 1987;10:363–401.

McKeefry DJ, Watson JD, Frackowiak RS, Fong K, Zeki S. The activity in human areas V1/V2, V3, and V5 during the perception of coherent and incoherent motion. *Neuroimage* 1997;5:1–12.

Meiboom S, Gill D. Modified spin echo method for measuring nuclear relaxation times. *Rev Sci Instrum* 1958;29:668.

Ogawa S, Lee TM, Kay AR, Tank DW. Brain magnetic resonance imaging with contrast dependent on blood oxygenation. *Proc Natl Acad Sci USA* 1990;87:9868–72.

Paradiso MA. Monkey business builds a bridge to the human brain [news; comment]. *Nat Neurosci* 1999;2:491–2.

- Paxinos G, Huang X-F, Toga AW. *The Rhesus Monkey Brain in Stereotaxic Coordinates*, First ed. London: Academic Press, 1999.
- Rees G, Friston K, Koch C. A direct quantitative relationship between the functional properties of human and macaque V5. *Nat Neurosci* 2000;3:716–23.
- Saito H, Yukiie M, Tanaka K, Hikosaka K, et al. Integration of direction signals of image motion in the superior temporal sulcus of the macaque monkey. *J Neurosci* 1986;6:145–57.
- Sereno MI. Brain mapping in animals and humans. *Curr Opin Neurobiol* 1998;8:188–94.
- Sereno MI, Allman JM. Cortical visual areas in mammals. In: Leventhal AG, editor. *The Neural Basis of Visual Function*. London: Macmillan, 1991:160–72.
- Sereno MI, Dale AM, Reppas JB, Kwong KK, et al. Borders of multiple visual areas in humans revealed by functional magnetic resonance imaging. *Science* 1995;268:889–93.
- Snyder LH, Batista AP, Andersen RA. Coding of intention in the posterior parietal cortex. *Nature* 1997;386:167–70.
- Stapleton SR, Kiriakopoulos E, Mikulis D, Drake JM, et al. Combined utility of functional MRI, cortical mapping, and frameless stereotaxy in the resection of lesions in eloquent areas of brain in children. *Pediatr Neurosurg* 1997;26:68–82.
- Stefanacci L, Reber P, Costanza J, Wong E, et al. fMRI of monkey visual cortex. *Neuron* 1998;20:1051–7.
- Tanaka K, Hikosaka K, Saito H, Yukiie M, et al. Analysis of local and wide-field movements in the superior temporal visual areas of the macaque monkey. *J Neurosci* 1986;6:134–44.
- Tootell RB, Dale AM, Sereno MI, Malach R. New images from human visual cortex. *Trends Neurosci* 1996;19:481–9.
- Tootell RB, Reppas JB, Kwong KK, Malach R, et al. Functional analysis of human MT and related visual cortical areas using magnetic resonance imaging. *J Neurosci* 1995;15:3215–30.
- Tootell RB, Switkes E, Silverman MS, Hamilton SL. Functional anatomy of macaque striate cortex. II. Retinotopic organization. *J Neurosci* 1988;8:1531–68.
- Ungerleider LG, Desimone R. Cortical connections of visual area MT in the macaque. *J Comp Neurol* 1986;248:190–222.
- Wood ML, Bronskill MJ, Mulkern RV, Santyr GE. Physical MR desktop data. *J Magn Reson Imaging (Suppl)* 1993;3:19–24.
- Zeki SM. Colour coding in rhesus monkey prestriate cortex. *Brain Res* 1973;53:422–7.
- Zeki S, Watson JD, Lueck CJ, Friston KJ, et al. A direct demonstration of functional specialization in human visual cortex. *J Neurosci* 1991;11:641–9.
- Zhang Z, Andersen AH, Avison MJ, Gerhardt GA, Gash DM. Functional MRI of apomorphine activation of the basal ganglia in awake rhesus monkeys. *Brain Res* 2000;852:290–6.